16th World Conference on Earthquake, 16WCEE 2017
Santiago Chile, January 9th to 13th 2017
Paper N° 3355 (Abstract ID)
Registration Code: S-G1462817691

SEISMIC DESIGN AND EVALUATION OF MOMENT RESISTING FRAMES USING ELASTOMERIC DAMPERS

C.A.Basagiannis[(1)], M.S. Williams[(2)]

[(1)] *DPhil Candidate, Department of Engineering Science, University of Oxford, Oxford, United Kingdom, christos.basagiannis@eng.ox.ac.uk*
[(2)] *Professor, Department of Engineering Science, University of Oxford, Oxford, United Kingdom, martin.williams@eng.ox.ac.uk*

Abstract

Passive energy dissipation mechanisms have the ability to enhance the dynamic performance of structures by reducing interstorey drifts and the inelastic deformation of the primary structural elements. The aim of the project of which this work forms a part is the experimental and analytical evaluation of elastomeric dampers (EDs) as passive energy dissipation devices. Elastomeric dampers consist of a rubbery material bonded between two steel plates; they have similar characteristics to viscoelastic dampers, but are less sensitive to frequency and temperature, a fact which make them more effective. This paper describes analytical and experimental research aimed at fully capturing the behaviour of a proprietary damper, developed by TARRC (the Tun Abdul Razak Research Centre, UK) and generating a numerical model of the damper for use in analysis and design. A modified Generalised Maxwell Model is shown to give an excellent fit to experimental test data. In addition, preliminary structural analyses using a simplified damper model show the potential benefits of elastomeric dampers on seismic performance.

Keywords: Elastomeric; Damper; Dissipation; Generalized Maxwell Model;

1. Introduction

Under earthquake ground motions and strong winds structures could experience high levels of vibrations and accelerations, leading to residual displacements and damage of primary structural elements, or even total collapse of the structure. Passive energy dissipation systems can significantly improve the seismic behaviour of structures by reducing accelerations and inelastic deformation demands on the primary elements. If carefully designed, these systems will slightly increase the initial building design cost and greatly improve the structure's performance under strong earthquakes.

The present paper is concerned with the modelling of elastomeric dampers (EDs) as passive energy dissipation devices, and the analysis of steel moment resisting frames enhanced with EDs. Elastomers, like ViscoElastic (VE) materials, have properties that depend on strain amplitude, frequency, and temperature. However, elastomers consist of much more complicated time domain behaviour with softening-hardening behaviour (Fig. 1), and cannot be easily modeled as linearly proportional to displacement and velocity, as in the VE material case. Typical EDs consist of layers of elastomer bonded between steel plates (Fig. 2), and they are devices for dissipating energy induced by either earthquakes or strong winds through shear deformation.

Regarding the modelling of VE dampers and EDs, most previous efforts were focused on the Maxwell model, Kelvin-Voigt model [1], Generalized Maxwell Model (GMM) [4], Fractional Derivatives model [5, 6], Modified Bouc-Wen model [4, 8], Boltzman superposition method [7], while a new model was also proposed by Lee [9]. One of the main characteristics of the elastomer is stress relaxation. However, the relaxation observed in the elastomeric materials can not be modelled by one Maxwell model, since it is usually broader than the predictions of the model [10]. Hence, while the simplicity of both Maxwell and Kelvin-Voigt models are attractive for design purposes, they cannot accurately predict the elastomer's characteristics [10]. The Generalized Maxwell Model and Fractional Derivatives model on the other hand can take into account multiple stress relaxations and could lead to more accurate results [10, 11].

Due to their complexity in the time domain, specific ways of determining the model parameters in the frequency domain have been used, through Laplace and Fourier transforms. According to these methods, the shear storage modulus and the loss factor are analytically determined for every frequency, and then are fitted to the experimental results, extracting the models' parameters. However, the fact that the analytical shear storage modulus can be close to the experimental one does not necessarily mean that the time domain behaviour of the elastomer can be described. Fig. 1 shows a typical example of this, comparing test results from VE and ED behaviour having almost identical shear storage modulus and loss factor. In spite of this apparent similarity, the hysteretic behaviour is clearly different. The same applies with the Fractional Derivative Model.

Herein, the concept of a Modified Generalized Maxwell Model (MGMM) is employed in the development of a force-displacement relationship for elastomeric dampers. Two elastomeric dampers provided by TARRC were tested over a range of strain amplitudes and frequencies, enabling optimal model parameters to be determined. The effect of adding EDs to a framed building was also investigated analytically.

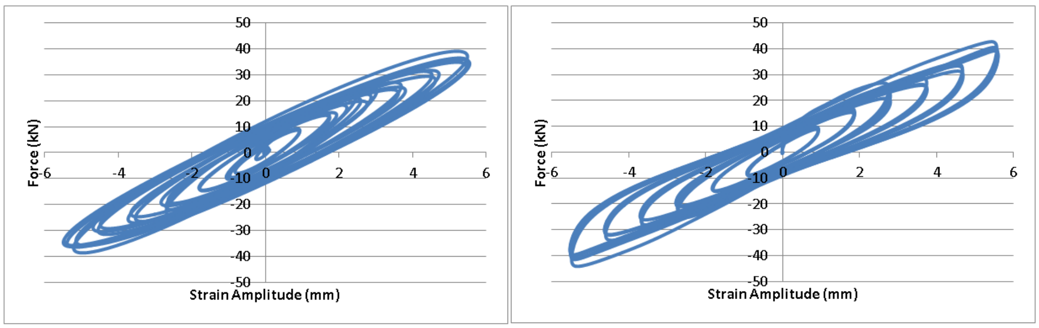

Fig. 1 – Force-Displacement Relationship: Comparison of VE behaviour (left), and Elastomeric behaviour (right)

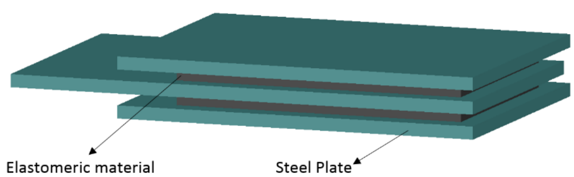

Fig. 2 – Typical Elastomeric Damper

2. Experimental Procedure and Results

Two elastomeric dampers were provided by the Tun Abdul Razak Research Centre (TARRC). They consist of a rubbery material bonded between steel plates. The overall dimensions of the rubber material are 230 mm in the longitudinal direction (coinciding with the loading direction), 180 mm in the transverse direction, and 11.75 mm width (Fig 3).

The two dampers were tested simultaneously in a symmetric arrangement; the overall setup of the rig is illustrated at Fig. 4. A thermocouple was attached to the elastomer in order to measure the ambient temperature, but also to capture any increase in temperature during the tests. A 100 kN servo-hydraulic actuator was used to evaluate the EDs' performance under a range of displacement amplitudes and frequencies. The first series of tests was the application of sinusoidal displacement histories at the EDs. Each history had 6 ramped cycles and 17 full sinusoidal cycles. This process was repeated for frequencies 0.25-4.0Hz, and for displacement amplitudes 10%-50% of the elastomer's thickness. The equivalent shear modulus and loss factors were obtained for every test and are summarized in Table 1 and Figs 5 and 6. It can be clearly seen that the dominant factor which affects the elastomer's dynamic behaviour is the amplitude and not the frequency, especially in the case of loss factor where it practically remains the same regardless any change in frequency. It is also noticeable that when the strain amplitude increases above 30% the shear storage modulus tends to a constant value.

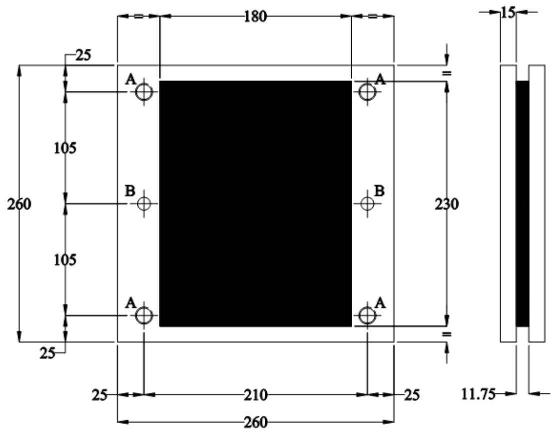

Fig. 3 – Dimensions of individual Elastomeric Damper-Dimensions are in mm

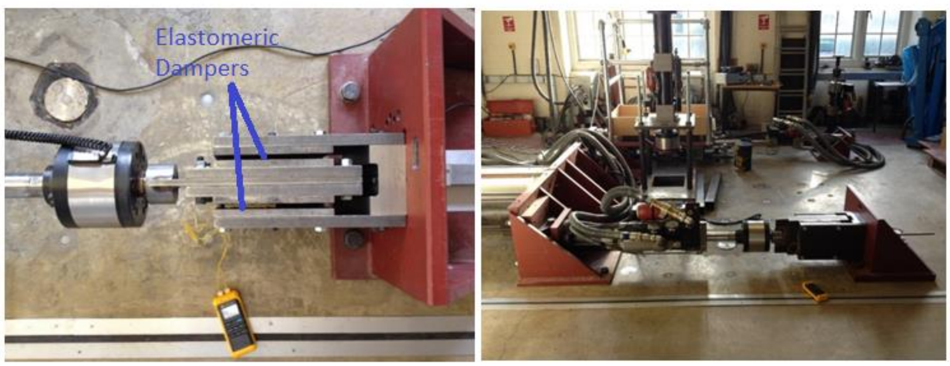

Fig. 4 – Final Design of the test rig

Table 1 – Mechanical Properties of the EDs

	f=0.25Hz		**f=0.5Hz**		**f=1Hz**		**f=2Hz**		**f=3Hz**		**f=4Hz**	
Shear Strain %	**Gs (Mpa)**	**n**	**Gs (Mpa)**	**n**	**Gs (Mpa)**	**n**	**Gs (Mpa)**	**n**	**Gs (Mpa)**	**n**	**Gs (Mpa)**	**n**
10	1.3574	0.4068	1.3604	0.4145	1.4645	0.4106	1.6048	0.4050	1.6939	0.4001	1.7582	0.3965
20	1.0412	0.3553	1.0723	0.3531	1.1449	0.3549	1.2363	0.3527	1.2988	0.3490	1.3419	0.3468
30	0.8739	0.3340	0.9139	0.3337	0.9706	0.3364	1.0486	0.3357	1.0905	0.3332	1.1203	0.3321
40	0.816	0.3362	0.8377	0.3282	0.8891	0.3310	0.9454	0.3318	0.9834	0.3285	1.0148	0.3266
50	0.7641	0.3016	0.7979	0.3055	0.8402	0.3095	0.8936	0.3105	0.9214	0.3112	0.9507	0.3085

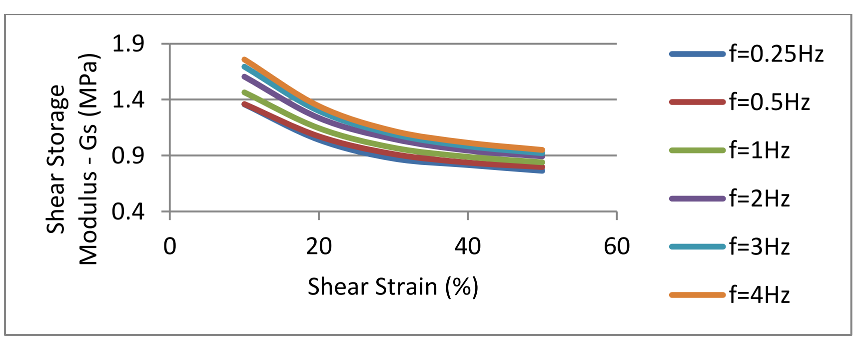

Fig. 5 – Shear Storage Modulus – Frequency and Amplitude Dependence

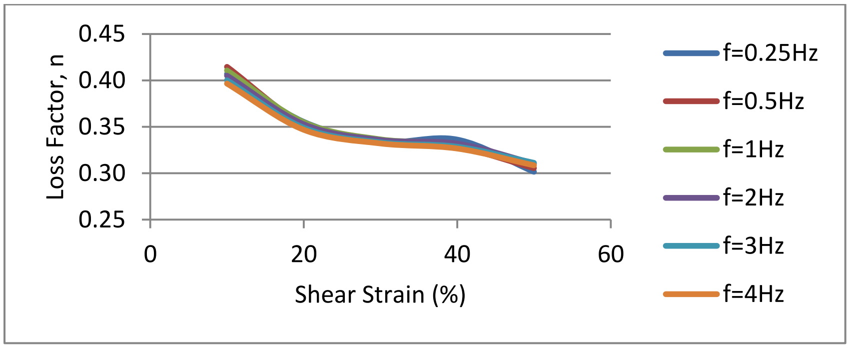

Fig. 6 – Loss factor – Frequency and Amplitude Dependence

3. Modified Generalized Maxwell Model (MGMM)

In this section we present the theory of the Generalised Maxwell Model, explain how it has been modified to provide an improved representation of ED behaviour, and present the model parameters derived from fitting to experimental data.

3.1 Linear Generalized Maxwell Model (GMM)

The linear Generalized Maxwell Model (GMM) consists of linear spring, with spring stiffness parameter called k_0, in parallel with N Maxwell elements (Fig 7). Although, it is very easy to extract the analytical force-displacement relationship when only one Maxwell element is used, things are becoming much more complicated when more than two elements are being used. A four-4 element GMM was used in this paper.

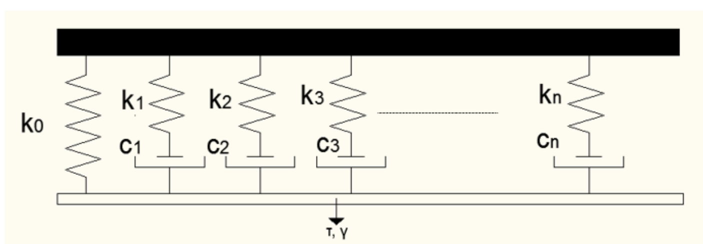

Fig. 3 – Linear Generalized Maxwell Model (GMM)

The time relaxation for the i_{th} Maxwell element is denoted, τ_i, and is equal to c_i/k_i. In the case of four Maxwell elements the total force is:

$$F = F_0 + F_1 + F_2 + F_3 + F_4 \quad (1)$$

From Eq. (1):

$$F_4 = F - F_1 - F_2 - F_3 - F_0 \quad (2)$$

where F is the total force applied at the GMM.
For every individual Maxwell element, *i*, the following equation can be derived:

$$\dot{F}_i = k_i \, \dot{u}_i - (k_i/c_i)F_i \quad (3)$$

where the dot denotes the differentiation with respect to time.
The first derivative of (1) gives:

$$\dot{F} = \dot{F}_0 + \dot{F}_1 + \dot{F}_2 + \dot{F}_3 + \dot{F}_4 \tag{4}$$

Substituting (3) into (4):

$$\dot{F} = \dot{F}_0 + k_1\,\dot{u}_1 - \left(\frac{k_1}{c_1}\right)F_1 + k_2\,\dot{u}_2 - \left(\frac{k_2}{c_2}\right)F_2 + k_3\dot{u}_3 - \left(\frac{k_3}{c_3}\right)F_3 + k_4\,\dot{u}_4 - \left(\frac{k_4}{c_4}\right)F_4 \tag{5}$$

In the GMM case, $u_1 = u_2 = u_3 = u_4 = u$. Hence, substituting from Eq. (2), Eq.(5) becomes:

$$\dot{F} = (k_1 + k_2 + k_3 + k_4)\,\dot{u} - \left(\frac{k_1}{c_1}\right)F_1 - \left(\frac{k_2}{c_2}\right)F_2 - \left(\frac{k_3}{c_3}\right)F_3 - \left(\frac{k_4}{c_4}\right)(F - F_1 - F_2 - F_3 - F_0) + \dot{F}_0 \tag{6}$$

which leads to:

$$\dot{F} = (k_1 + k_2 + k_3 + k_4)\,\dot{u} + F_1\left(\frac{k_4}{c_4} - \frac{k_1}{c_1}\right) + F_2\left(\frac{k_4}{c_4} - \frac{k_2}{c_2}\right) + F_3\left(\frac{k_4}{c_4} - \frac{k_3}{c_3}\right) - \frac{k_4}{c_4}F + \frac{k_4}{c_4}F_0 + \dot{F}_0 \tag{7}$$

Solving for the F_3 term:

$$F_3\left(\frac{k_4}{c_4} - \frac{k_3}{c_3}\right) = \dot{F} - (k_1 + k_2 + k_3 + k_4)\,\dot{u} - F_1\left(\frac{k_4}{c_4} - \frac{k_1}{c_1}\right) - F_2\left(\frac{k_4}{c_4} - \frac{k_2}{c_2}\right) + \frac{k_4}{c_4}F - \frac{k_4}{c_4}F_0 - \dot{F}_0 \tag{8}$$

Differentiating Eq. (7):

$$\ddot{F} = (k_1 + k_2 + k_3 + k_4)\,\ddot{u} + \dot{F}_1\left(\frac{k_4}{c_4} - \frac{k_1}{c_1}\right) + \dot{F}_2\left(\frac{k_4}{c_4} - \frac{k_2}{c_2}\right) + \dot{F}_3\left(\frac{k_4}{c_4} - \frac{k_3}{c_3}\right) - \frac{k_4}{c_4}\dot{F} + \frac{k_4}{c_4}\dot{F}_0 + \ddot{F}_0 \tag{9}$$

Using Eq. (3) for elements 1, 2, and 3:

$$\dot{F}_1 = k_1\,\dot{u} - (k_1/c_1)F_1 \tag{10}$$

$$\dot{F}_2 = k_2\,\dot{u} - (k_2/c_2)F_2 \tag{11}$$

$$\dot{F}_3 = k_3\,\dot{u} - (k_3/c_3)F_3 \tag{12}$$

Combining Eq. (9), (10), (11), and (12):

$$\begin{aligned}\ddot{F} = {} & (k_1 + k_2 + k_3 + k_4)\,\ddot{u} + k_1\,\dot{u}\left(\frac{k_4}{c_4} - \frac{k_1}{c_1}\right) - \frac{k_1}{c_1}F_1\left(\frac{k_4}{c_4} - \frac{k_1}{c_1}\right) + k_2\,\dot{u}\left(\frac{k_4}{c_4} - \frac{k_2}{c_2}\right) - \frac{k_2}{c_2}F_2\left(\frac{k_4}{c_4} - \frac{k_2}{c_2}\right) + \\ & k_3\,\dot{u}\left(\frac{k_4}{c_4} - \frac{k_3}{c_3}\right) - \frac{k_3}{c_3}F_3\left(\frac{k_4}{c_4} - \frac{k_3}{c_3}\right) - \frac{k_4}{c_4}\dot{F} + \frac{k_4}{c_4}\dot{F}_0 + \ddot{F}_0\end{aligned} \tag{13}$$

Substituting Eq. (8) into (13):

$$\begin{aligned}\ddot{F} = {} & (k_1 + k_2 + k_3 + k_4)\,\ddot{u} + \left(\frac{k_3}{c_3} + \frac{k_4}{c_4}\right)(k_1 + k_2 + k_3 + k_4)\dot{u} - \left(\frac{k_1}{c_1}k_1 + \frac{k_2}{c_2}k_2 + \frac{k_3}{c_3}k_3 + \frac{k_4}{c_4}k_4\right)\dot{u} + \\ & F_2\left(\frac{k_4}{c_4} - \frac{k_2}{c_2}\right)\left(\frac{k_3}{c_3} - \frac{k_2}{c_2}\right) + F_1\left(\frac{k_4}{c_4} - \frac{k_1}{c_1}\right)\left(\frac{k_3}{c_3} - \frac{k_1}{c_1}\right) - \left(\frac{k_3}{c_3} + \frac{k_4}{c_4}\right)\dot{F} - \left(\frac{k_3}{c_3}\frac{k_4}{c_4}\right)F + \left(\frac{k_3}{c_3} + \frac{k_4}{c_4}\right)\dot{F}_0 + \\ & \left(\frac{k_3}{c_3}\frac{k_4}{c_4}\right)F_0 + \ddot{F}_0\end{aligned} \tag{14}$$

Carrying out the same procedure for the 3rd, and 4th derivative of Eq. (7), the following force-displacement relationship of the GMM for four elements can be determined:

$$F + \left(\frac{c_1}{k_1} + \frac{c_2}{k_2} + \frac{c_3}{k_3} + \frac{c_4}{k_4}\right)\dot{F} + \left(\frac{c_1}{k_1}\frac{c_2}{k_2} + \frac{c_1}{k_1}\frac{c_3}{k_3} + \frac{c_1}{k_1}\frac{c_4}{k_4} + \frac{c_2}{k_2}\frac{c_3}{k_3} + \frac{c_2}{k_2}\frac{c_4}{k_4} + \frac{c_3}{k_3}\frac{c_4}{k_4}\right)\ddot{F} +$$
$$\left(\frac{c_1}{k_1}\frac{c_2}{k_2}\frac{c_3}{k_3} + \frac{c_1}{k_1}\frac{c_2}{k_2}\frac{c_4}{k_4} + \frac{c_1}{k_1}\frac{c_3}{k_3}\frac{c_4}{k_4} + \frac{c_2}{k_2}\frac{c_3}{k_3}\frac{c_4}{k_4}\right)\dddot{F} + \left(\frac{c_1}{k_1}\frac{c_2}{k_2}\frac{c_3}{k_3}\frac{c_4}{k_4}\right)F^{4,t} =$$
$$(c_1 + c_2 + c_3 + c_4)\dot{u} +$$
$$\left\{\left(\frac{c_1}{k_1}\frac{c_2}{k_2}\right)(k_1 + k_2) + \frac{c_1}{k_1}\frac{c_3}{k_3}(k_1 + k_3) + \frac{c_1}{k_1}\frac{c_4}{k_4}(k_1 + k_4) + \frac{c_2}{k_2}\frac{c_3}{k_3}(k_2 + k_3) + \frac{c_2}{k_2}\frac{c_4}{k_4}(k_2 + k_4) + \frac{c_3}{k_3}\frac{c_4}{k_4}(k_3 + k_4)\right\}\ddot{u} +$$
$$\left\{\left(\frac{c_1}{k_1}\frac{c_2}{k_2}\frac{c_3}{k_3}\right)(k_1 + k_2 + k_3) + \frac{c_1}{k_1}\frac{c_2}{k_2}\frac{c_4}{k_4}(k_1 + k_2 + k_4) + \frac{c_1}{k_1}\frac{c_3}{k_3}\frac{c_4}{k_4}(k_1 + k_3 + k_4) + \frac{c_2}{k_2}\frac{c_3}{k_3}\frac{c_4}{k_4}(k_2 + k_3 + k_4)\right\}\dddot{u} +$$
$$\left(\frac{c_1}{k_1}\frac{c_2}{k_2}\frac{c_3}{k_3}\frac{c_4}{k_4}\right)(k_1 + k_2 + k_3 + k_4)u^{4,t} +$$
$$F_0 + \left(\frac{c_1}{k_1} + \frac{c_2}{k_2} + \frac{c_3}{k_3} + \frac{c_4}{k_4}\right)(\dot{F}_0) + \left(\frac{c_1}{k_1}\frac{c_2}{k_2} + \frac{c_1}{k_1}\frac{c_3}{k_3} + \frac{c_1}{k_1}\frac{c_4}{k_4} + \frac{c_2}{k_2}\frac{c_3}{k_3} + \frac{c_2}{k_2}\frac{c_4}{k_4} + \frac{c_3}{k_3}\frac{c_4}{k_4}\right)(\ddot{F}_0) +$$
$$\left(\frac{c_1}{k_1}\frac{c_2}{k_2}\frac{c_3}{k_3} + \frac{c_1}{k_1}\frac{c_2}{k_2}\frac{c_4}{k_4} + \frac{c_1}{k_1}\frac{c_3}{k_3}\frac{c_4}{k_4} + \frac{c_2}{k_2}\frac{c_3}{k_3}\frac{c_4}{k_4}\right)(\dddot{F}_0) + \left(\frac{c_1}{k_1}\frac{c_2}{k_2}\frac{c_3}{k_3}\frac{c_4}{k_4}\right)(F_0^{4,t}) \quad (15)$$

where $F_0^{4,t}$ denotes for the 4^{th} derivative of the force F_0.

3.2 Modified Generalized Maxwell Model (MGMM)

Both the GMM, and the Generalized Derivatives methods can be valid only for pure VE behaviour, which can take into account multiple time relaxations. However, they are not adequate to describe any nonlinear characteristics of elastomers. In order to take these into account, the nonlinear terms au^b, and $c\dot{u}^d$ will be used in addition to the four-element GMM. Finally, a linear dashpot will be added into the force F_0. Therefore, the final model describing the force-displacement relationship can be divided into four parts:

1) The linear GMM obtained from equation (15)
2) A linear dashpot, so the total force F_0 equals with $k_0 u + c_0 \dot{u}$
3) The nonlinear term au^b
4) The nonlinear term $c\dot{u}^d$

These four individual parts lead to:

$$F + \left(\frac{c_1}{k_1} + \frac{c_2}{k_2} + \frac{c_3}{k_3} + \frac{c_4}{k_4}\right)\dot{F} + \left(\frac{c_1}{k_1}\frac{c_2}{k_2} + \frac{c_1}{k_1}\frac{c_3}{k_3} + \frac{c_1}{k_1}\frac{c_4}{k_4} + \frac{c_2}{k_2}\frac{c_3}{k_3} + \frac{c_2}{k_2}\frac{c_4}{k_4} + \frac{c_3}{k_3}\frac{c_4}{k_4}\right)\ddot{F} +$$
$$\left(\frac{c_1}{k_1}\frac{c_2}{k_2}\frac{c_3}{k_3} + \frac{c_1}{k_1}\frac{c_2}{k_2}\frac{c_4}{k_4} + \frac{c_1}{k_1}\frac{c_3}{k_3}\frac{c_4}{k_4} + \frac{c_2}{k_2}\frac{c_3}{k_3}\frac{c_4}{k_4}\right)\dddot{F} + \left(\frac{c_1}{k_1}\frac{c_2}{k_2}\frac{c_3}{k_3}\frac{c_4}{k_4}\right)F^{4,t} =$$
$$(c_1 + c_2 + c_3 + c_4)\dot{u} +$$
$$\left\{\left(\frac{c_1}{k_1}\frac{c_2}{k_2}\right)(k_1 + k_2) + \frac{c_1}{k_1}\frac{c_3}{k_3}(k_1 + k_3) + \frac{c_1}{k_1}\frac{c_4}{k_4}(k_1 + k_4) + \frac{c_2}{k_2}\frac{c_3}{k_3}(k_2 + k_3) + \frac{c_2}{k_2}\frac{c_4}{k_4}(k_2 + k_4) + \frac{c_3}{k_3}\frac{c_4}{k_4}(k_3 + k_4)\right\}\ddot{u} +$$
$$\left\{\left(\frac{c_1}{k_1}\frac{c_2}{k_2}\frac{c_3}{k_3}\right)(k_1 + k_2 + k_3) + \frac{c_1}{k_1}\frac{c_2}{k_2}\frac{c_4}{k_4}(k_1 + k_2 + k_4) + \frac{c_1}{k_1}\frac{c_3}{k_3}\frac{c_4}{k_4}(k_1 + k_3 + k_4) + \frac{c_2}{k_2}\frac{c_3}{k_3}\frac{c_4}{k_4}(k_2 + k_3 + k_4)\right\}\dddot{u} +$$
$$\left(\frac{c_1}{k_1}\frac{c_2}{k_2}\frac{c_3}{k_3}\frac{c_4}{k_4}\right)(k_1 + k_2 + k_3 + k_4)u^{4,t} +$$
$$(k_0 u + c_0 \dot{u}) + \left(\frac{c_1}{k_1} + \frac{c_2}{k_2} + \frac{c_3}{k_3} + \frac{c_4}{k_4}\right)(k_0 \dot{u} + c_0 \ddot{u}) + \left(\frac{c_1}{k_1}\frac{c_2}{k_2} + \frac{c_1}{k_1}\frac{c_3}{k_3} + \frac{c_1}{k_1}\frac{c_4}{k_4} + \frac{c_2}{k_2}\frac{c_3}{k_3} + \frac{c_2}{k_2}\frac{c_4}{k_4} + \frac{c_3}{k_3}\frac{c_4}{k_4}\right)(k_0 \ddot{u} + c_0 \dddot{u}) +$$
$$\left(\frac{c_1}{k_1}\frac{c_2}{k_2}\frac{c_3}{k_3} + \frac{c_1}{k_1}\frac{c_2}{k_2}\frac{c_4}{k_4} + \frac{c_1}{k_1}\frac{c_3}{k_3}\frac{c_4}{k_4} + \frac{c_2}{k_2}\frac{c_3}{k_3}\frac{c_4}{k_4}\right)(k_0 \dddot{u} + c_0 u^{4,t}) + \left(\frac{c_1}{k_1}\frac{c_2}{k_2}\frac{c_3}{k_3}\frac{c_4}{k_4}\right)(k_0 u^{4,t} + c_0 u^{5,t}) + au^b + c\dot{u}^d \quad (16)$$

3.3 Determination of MGMM constants

In order to determine the parameters of Eq. (16), sweep amplitude sinusoidal tests were carried out for each frequency. The Levenberg-Marquardt algorithm was then used to minimize the error between the experimental values and the force from the model [12]. Simultaneous minimization of all of these tests was carried out and the final parameters are presented in Table 2. Typical examples of comparison between the experimental and analytical data in time domain are shown in Figs. 7, and 8, and they validate the model, since the results are in very good agreement with the experimental ones.

Table 2 – ED model parameters

k1 (kN/mm)	k2 (kN/mm)	k3 (kN/mm)	k4 (kN/mm)	c1 (kNsec/mm)	c2 (kNsec/mm)	c3 (kNsec/mm)
0.94253302	1.324481681	0.202842651	0.672119685	0.005759064	0.007912148	0.001188418
c4 (kNsec/mm)	**k0 (kN/mm)**	**c0 (kNsec/mm)**	**a(kN/mm)**	**b**	**c(kNsec/mm)**	**d**
0.029552529	1.939293993	0.086939566	4.188734089	0.836567428	2.748318103	0.448747969

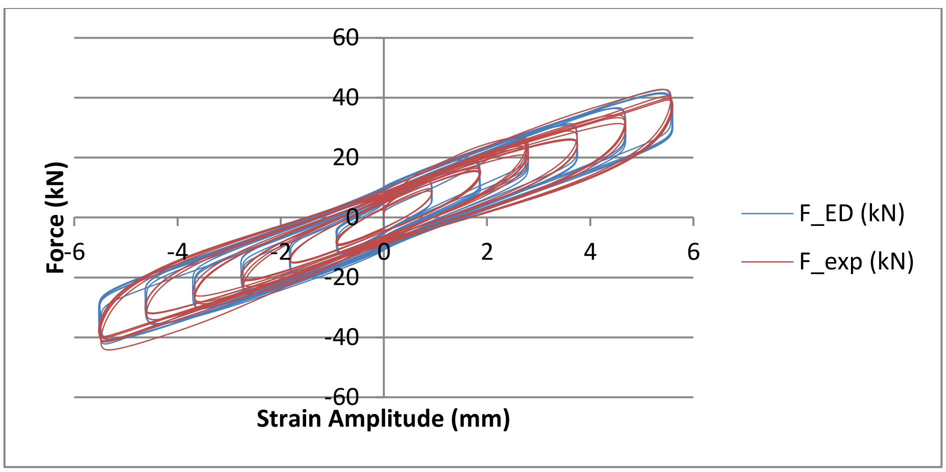

Fig. 7 – Comparison of force between experiment and model for sweep amplitude test for 2Hz

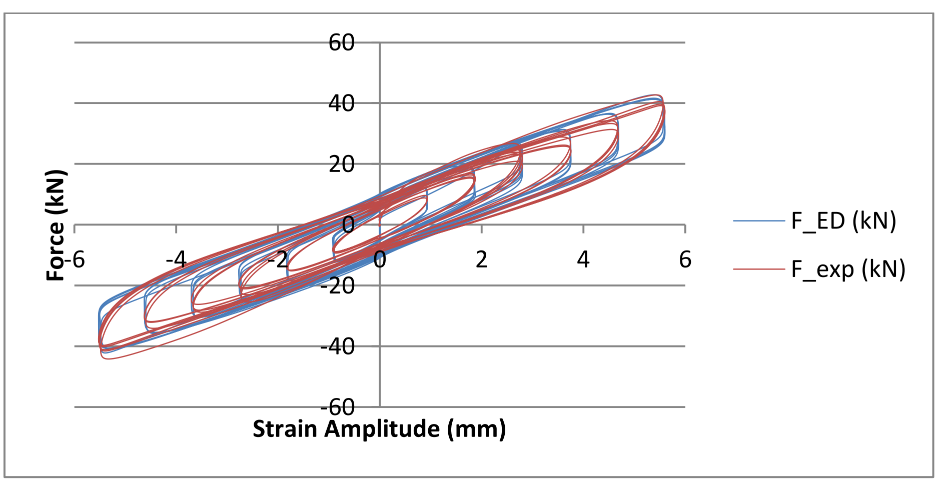

Fig. 8 – Comparison of force between experiment and model for sweep amplitude test for 0.5Hz

4. Analysis

To evaluate the effectiveness of EDs in improving the seismic performance of buildings, a series of analyses were performed on a specimen frame model, with and without dampers. In the early analyses reported here, a simple damper model was used. Work currently in progress is modifying this to MGMM model presented above. Fig. 9 shows the plan of a 10 storey, 4 by 3 bays steel frame which was used in this study. The design of this building was carried out according to EC8. More specifically, in one of the main directions of the frame structure, concentric diagonal braces were installed in order to resist the horizontal forces, while moment resisting frames were the main dissipation mechanism in the other direction. The building was characterised as DCM (Ductility Class Medium), and a behaviour factor, q equal to 4 was used in both directions. To examine the effect of elastomeric dampers on the seismic performance of simple-conventional moment resisting frames (CMRFs), only the perimeter frames of the prototype building were used (Fig. 9). The finite element (FE) software SAP2000 was first used [13] for the three dimension design of the prototype steel structure, and the FE software OpenSees [14] was later used for the 2D nonlinear analysis of the perimeter MRF. In the latter case, elastomeric dampers and diagonal braces were also incorporated into the 2D CMRF. The steel sections used for each floor for the perimeter frame are shown in Table 3. The CMRF satisfies the capacity design concept (strong column-weak beam) and the maximum drift requirement of EC8. The dampers used in this study were modelled as simple viscoelastic materials, with an equivalent stiffness, k_{eq}, and a dashpot coefficient c_{eq}, based on the characterization tests carried out at Oxford University Dynamic Lab.

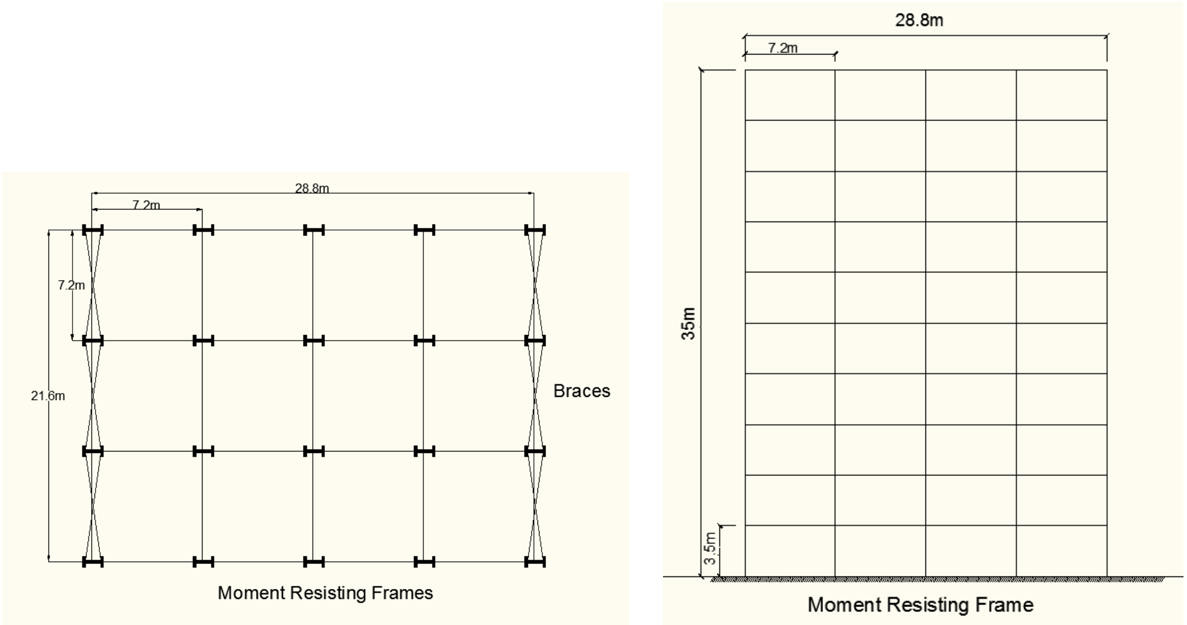

Figure 9: Left)Plan of 3D Steel Structure, Right) Perimeter Steel Moment Resisting Frame

Table 3: Steel Sections

Storeys	Column Section	Beam Section
1 - 4	HEB450	IPE400
5 - 7	HEB360	IPE360
8 - 10	HEB320	IPE330

4.1 Scaling Ground Motions

In this study the ground motions which were used are: a) ElCentro, b) ChiChi/CHY029-V, and c) Loma Prieta/WAH000. These records have been selected from PEER Ground Motion Database. However, in order for Eurocode 8 conditions to be satisfied a scaling procedure proposed by Fahjan [15] was selected. The scope of this method is to gradually match the response spectrum of EC8, by increasing some components of the ground motion spectrum index, and reducing some others. In essence, this method does not create new ground motions, but it modifies selected records in order to satisfy the above criteria. Hence, the response spectrum of the selected ground motions have been determined and are illustrated in Fig. 10, and 11, before and after the implementation of scaling procedure. There is a very good agreement between the scaled response spectrum and the one from EC8, especially in the range $0.2T_1$-$2T_1$, where the main interest is.

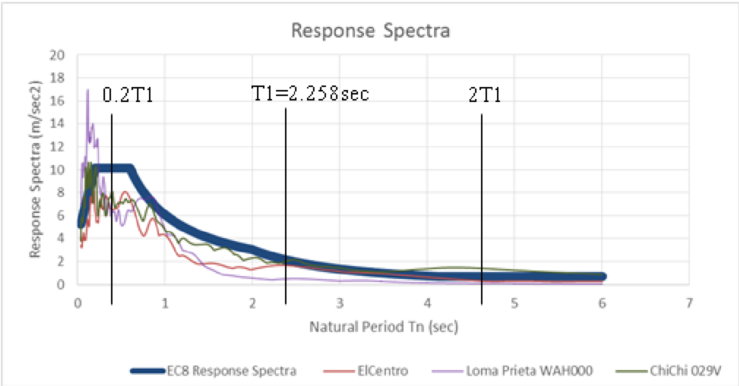

Figure 10: Response Spectrum of the original ground motions

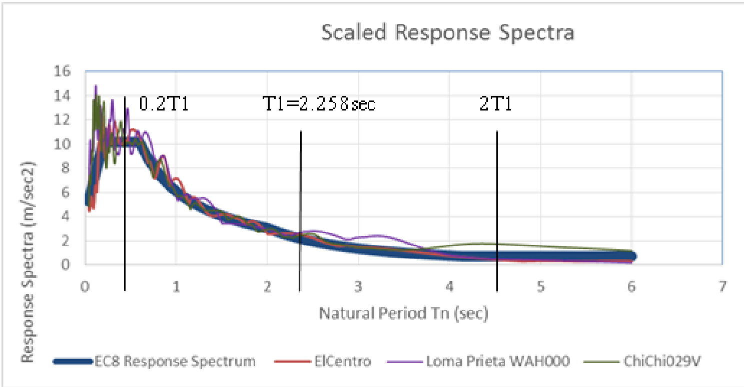

Figure 11: Response Spectrum of the scaled ground motions

4.2 Seismic Response

2D nonlinear models were developed in order to evaluate the effect of elastomeric dampers on CMRFs, with the FE software OpenSees. The beams and columns were modelled as distributed plasticity nonlinear elements, with fiber sections. A Rayleigh damping matrix was used to model inherent damping of 2% at the first two modes of vibration. Regarding the representation of the elastomeric damper, concentric diagonal dampers were added to the initial CMRF, using zero length elements connected between the top of the braces and the middle of the beams. A combination of spring and dashpot in parallel was assigned to the zero length element, also known and as Kelvin-Voigt model. As it is shown in Fig. 12, EDs were added at the first and last bay of the perimeter CMRF, in order to improve its seismic performance. This addition led to a natural period decrease, from 2.258 seconds to 1.754 seconds (22%). Taking into account the worst case scenario, a frequency of 0.5 Hz was assumed (very close to the natural frequency of the structure after the implementation of the dampers) in order to assign an equivalent stiffness, k_{eq}=6.44 kN/mm, and an equivalent dashpot c_{eq}=0.684 kNsec/m based on the characterization tests.

The structure was tested under the scaled ElCentro ground motion for the Design Basis Earthquake (DBE), and the Maximum Considered Earthquake (MCE) (=1.5×DBE), and the results are illustrated in the following figures. Figs 13, 14, and 15 compare the roof drift time histories and the inter-storey shear forces of the CMRF and the DMRF (Damped Moment Resisting Frame), under the ElCentro ground motion scaled to the DBE and the MCE respectively. It was noticed that in the case of the CMRF, even for the DBE, there is a substantial residual displacement (16cm), with a maximum displacement of 55 cm, and excessive yielding in almost all beams and at the base of the first floor columns. Regarding the MCE, the yielding has spread not only to the base columns, but to other floor's columns as well, and to every beam. When EDs were added, then the residual drifts dropped almost to zero, while the maximum displacements were reduced by 35% for the DBE, and 40% for the MCE. Finally, the dispacement time history of the damper of the left bay of the 1st storey under the scaled ElCentro ground motion (DBE) was used as command displacement in the EDs in the lab, in order to give greater confidence in the analytical model (Fig. 16). Again the results show that the analytical model can accurately predict the EDs dynamic behaviour.

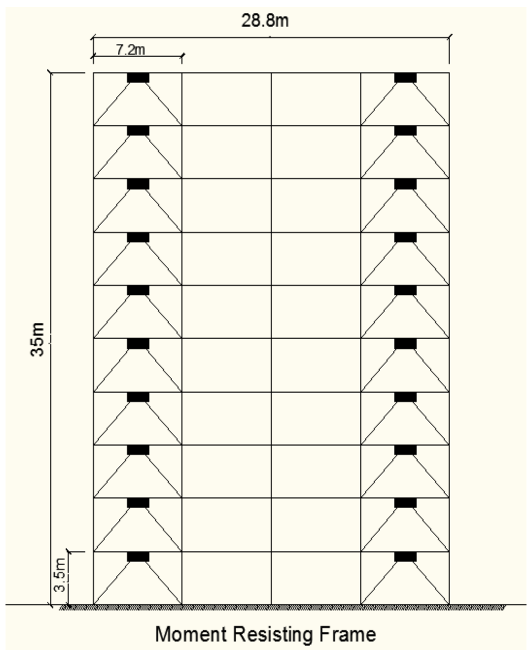

Figure 12: CMRF with Elastomeric Dampers

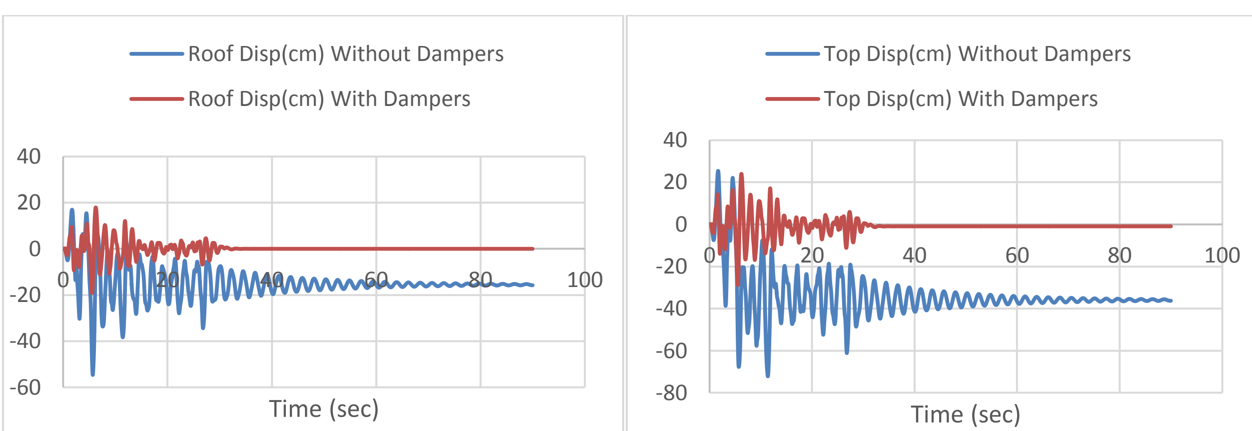

Figure 13: Roof Displacement of CMRF and DMRF for: Left)DBE, Right)MCE

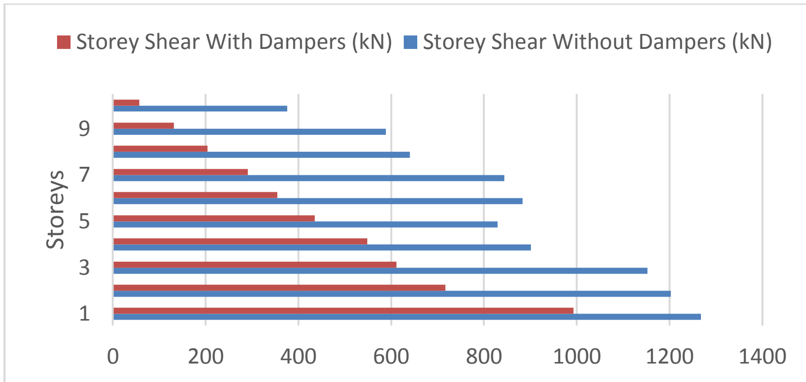

Figure 14: Interstorey Shear Forces of CMRF and DMRF for DBE

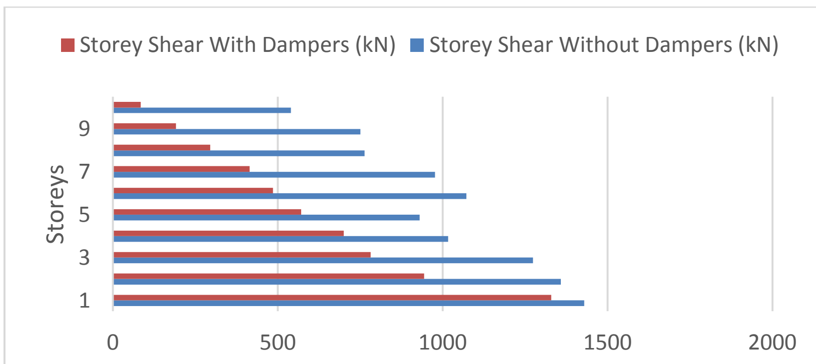

Figure 15: Interstorey Shear Forces of CMRF and DMRF for MCE

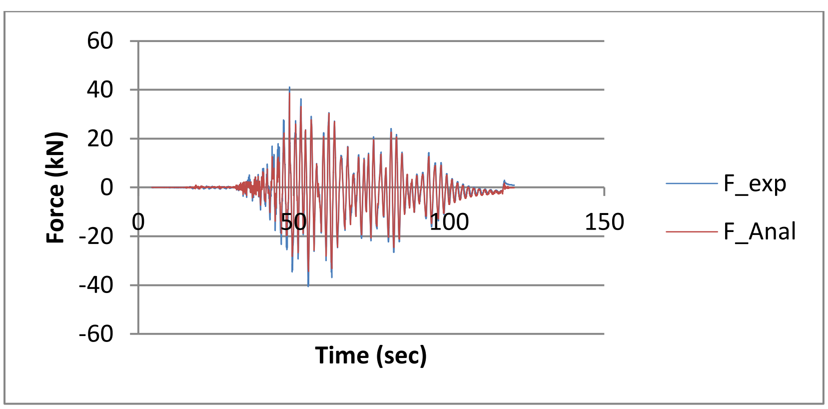

Figure 16: Displacements Time History based on DBE

5. Conclusions

A nonlinear numerical model was presented in order to represent the dynamic behaviour of elastomeric dampers. The model composed of a four-element Generalized Maxwell Model, combined with nonlinear parameters. This allowed both the time relaxations observed in the material and any nonlinearities to be taken into account. It is well known that the elastomer's behaviour depends on frequency, and strain amplitude. Hence, a series of tests has been carried out under a range of frequencies and strain amplitude, so the mechanical characteristics of the ED could be determined. Also, sweep amplitude tests were used to optimize the parameters of the model, which was found to be in a very good agreement with the experimental results.

The finite element software OpenSees was used for analytical purposes, where a 2D 10 storey – 4 bay CMRF was modelled. Later, sinplified models of elastomeric dampers were added at the frame throughout the building's height, and nonlinear time history analyses were carried out for both DBE, and MCE. For reasons of simplicity, a simple Kelvin-Voigt model was used to represent the ED, based on the mechanical characteristics obtained from the experiments; this will be improved upon in future analytical work. In terms of displacements, the DMRF exhibited very satisfactory seismic behaviour, and the Operational Performance level was achieved for both DBE and MCE. Furthermore, while the interstorey shear forces were greatly reduced, the base shear forces exhibited the smallest reduction (21% for DBE, and 7.1% for MCE). It should be mentioned that all the above results and the analyses are based on the assumption that the structure has been designed according to EC8, with anti-seismic protection. However, this is not the case for old steel structures which have insufficient strength and ductility, and often have been designed only to resist the gravity loads.

Summarizing, the numerical model developed in this study was able to capture the dynamic behaviour of the EDs obseved in experiments, while structural modelling showed that the EDs had beneficial effects on conventional steel frame buildings.

6. References

[1] Soong T.T., Dargush G.F. (1997): Passive Energy Dissipation Systems in Structural Engineering, *John Wiley & Sons, England*

[2] Lee, K.S. (2003): Seismic Behavior of Structures with Dampers Made from Ultra High Damping Natural Rubber - *Ph.D. Dissertation, Department of Civil and Environmental Engineering, Lehigh University*

[3] Fan C.P. (1998). Seismic Analysis, Behavior, and Retrofit of Non-Ductile Reinforced Concrete Frame Buildings with Viscoelastic Dampers, Ph.D. Dissertation, *Department of Civil and Environmental Engineering, Lehigh University*.

[4] Karavasilis T., Sause R., Ricles J., (2012): Seismic design and evaluation of steel moment-resisting frames with compressed elastomer dampers, *Journal of Earthquake Engineering and Structural Dynamics Journal*, 41:411-429

[5] Makris N., Dargush G.F., Constantinou M.C. (1993): Dynamic Analysis of Generalized Viscoelastic Fluids. *Journal of Engineering Mechanics,* **119,** 1663-1679

[6] Koh C. G., Kelly J.M. (1989): Application of Fractional Derivatives to Seismic Analysis of Base-Isolated models, *Journal of Earthquake Engineering and Structural Dynamics*, **19**:229-241

[7] Shen K.L., Soong T.T.(1995): Modeling of Viscoelastic Dampers for Structural Applications, *Journal of Engineering Mechanics,* **121,** 694-701

[8] Karavasilis T.L., Ricles J.M., Sause R., Chen C. (2011), "Experimental evaluation of the seismic performance of steel MRFs with compressed elastomer dampers using large-scale real-time hybrid simulation", *Journal of Engineering Structures:* **33** (2011) 1859–1869

[9] Lee, K.S. (2003): Seismic Behavior of Structures with Dampers Made from Ultra High Damping Natural Rubber, Ph.D. Dissertation, Department of Civil and Environmental Engineering, Lehigh University

[10] McCrum N.G., Buckley C.P., Bucknall C.B. (1997): Principles of Polymer Engineering, Second Edition, Oxford University Press

[11] Nashif A.D., Jones D.I.G., Henderson, J.P. (1985): Vibration Damping, John Wiley &Sons Inc

[12] MATLAB. A registered trademark of the math works, Inc. 2007.http://www.mathworks.com

[13] SAP2000. Static and dynamic finite element analysis of structures. Version9.1.4. Berkeley, California, USA: Computers and Structures Inc.; 2005

[14] OpenSees finite element software framework for developing applications to simulate the performance of structural and geotechnical systems subjected to earthquakes

[15] Fahjan Y.M., Ozdemir Z. (2008) "Scaling of earthquake accelerograms for non-linear dynamic analyses to match the earthquake design spectrum", *The 14th World Conference on Earthquake Engineering*, October 12-17, 2008, Beijing, China